Accepted Manuscript

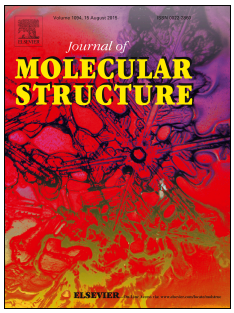

Intermolecular interactions in the solid state structures of neutral and *N*-protonated 5-alkoxymethyl-8-hydroxyquinolines

Mathias M. Schulze, Uwe Böhme, Anke Schwarzer, Edwin Weber

PII: S0022-2860(16)31282-0

DOI: 10.1016/j.molstruc.2016.11.090

Reference: MOLSTR 23191

To appear in: *Journal of Molecular Structure*

Received Date: 19 October 2016

Revised Date: 25 November 2016

Accepted Date: 28 November 2016

Please cite this article as: M.M. Schulze, U. Böhme, A. Schwarzer, E. Weber, Intermolecular interactions in the solid state structures of neutral and *N*-protonated 5-alkoxymethyl-8-hydroxyquinolines, *Journal of Molecular Structure* (2016), doi: 10.1016/j.molstruc.2016.11.090.

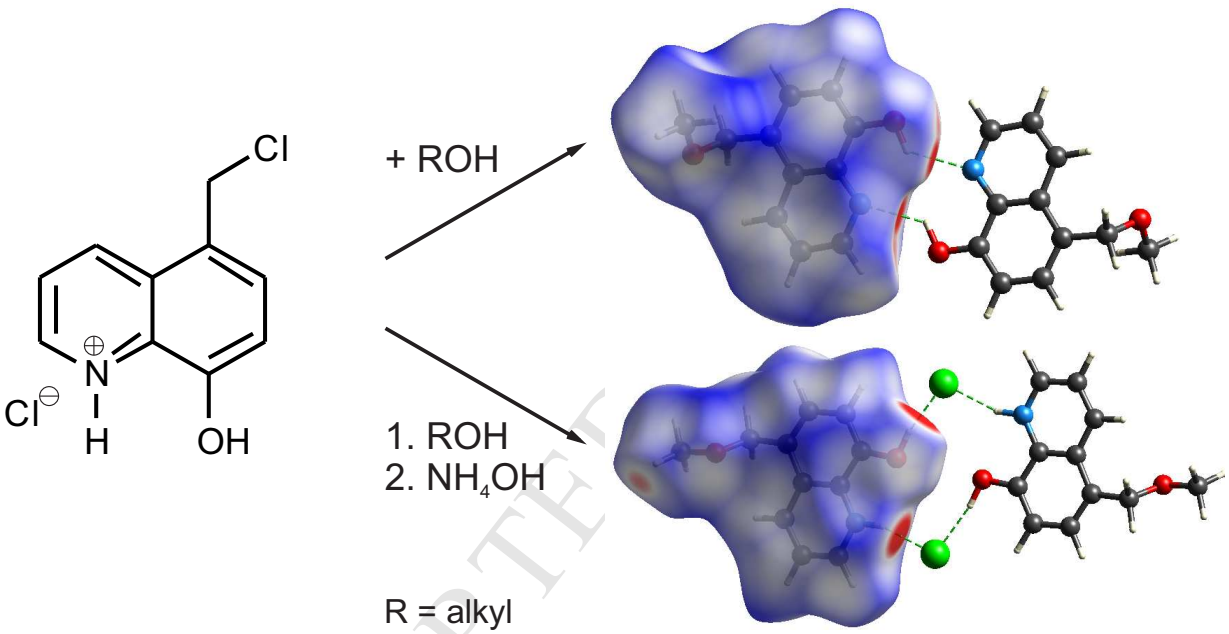

Intermolecular interactions in the solid state structures of neutral and *N*-protonated 5-alkoxymethyl-8-hydroxyquinolines

Mathias M. Schulze,[a] Uwe Böhme,[b] Anke Schwarzer,[a,*] Edwin Weber[a]

[a] *Institut für Organische Chemie, Technische Universität Bergakademie Freiberg, Leipziger Straße 29, D-09599 Freiberg/Sachsen, Germany*

[b] *Institut für Anorganische Chemie, Technische Universität Bergakademie Freiberg, Leipziger Straße 29, D-09599 Freiberg/Sachsen, Germany*

* Corresponding author. Tel.: +49 3731-393075; fax: +49 3731-393170.

E-mail address: anke.schwarzer@chemie.tu-freiberg.de.

Abstract

A series of five different alkoxymethyl substituted derivatives of 8-hydroxyquinoline was synthesised both in protonated (**1a-1e**) and neutral (**2a-2e**) form. The alkoxymethyl groups are MeO (**1a**, **2a**), EtO (**1b**, **2b**), *n*-PrO (**1c**, **2c**), *iso*-PrO (**1d**, **2d**), *n*-BuO (**1e**, **2e**). The compounds were characterised by single crystal X-ray diffraction and spectroscopic methods. Hirshfeld surface analysis was performed to analyse the crystal packing quantitatively. Topological analysis of the electron density distribution delivers information about the strength of the hydrogen bonds. The overall results reveal a main difference between the charged (**1a**-**1d**) and uncharged (**2a**-**2e**) compounds in the orientation of the hydroxyl group resulting in a different cyclic dimer formation. In both cases the structures are dominated by hydrogen bonding (**1a**-**1d**: O-H···Cl, N-H···Cl and **2a**-**2e**: O-H···N). Furthermore, all crystal structures show π involved interactions though taking only a minor part in the packing of the molecules.

Keywords: 8-hydroxyquinoline, alkoxymethyl substitution, crystal structure, Hirshfeld surface analysis, DFT, QTAIM, hydrogen bonding

1. Introduction

8-Hydroxyquinoline represents an important compound in the pharmacological chemistry[1] but is mostly known due to the versatile behaviour of forming metal complexes.[2,3,4] Hundreds of structures being composed of metal chelates derived from 8-hydroxyquinoline have been studied over the years,[2] and in many cases 8-hydroxyquinoline was used to design aprotic oligodendate ligands for the complexation of metal ions[5] and uncharged molecules[6]. Several reports confirm that 8-hydroxyquinoline can extensively be applied to the fluorogenic determination of cations.[7,8] Related complexes have been shown to serve as emissive materials in the emerging display technology based on organic light emitting diodes.[9] Moreover, 8-hydroxyquinoline has become an interesting compound in the development of electroluminescent materials both from experimental and theoretical viewpoints.[10,11] In the course of future applications, aspects of crystal engineering[12] based on corresponding compounds come into focus. Hence, we became interested to study the structural influence exercised on the solid state behaviour of a simple derivative of 8-hydroxyquinoline both by protonation and the insertion of different substituents, carried out by the compound series **1a**-**1e** and **2a**-**2e** (Scheme 1). We report crystal structures and comparatively discuss respective packing properties including demonstration of specific conformations and interaction motifs supported by the outcome of Hirshfeld surface analyses and quantum mechanical calculations.

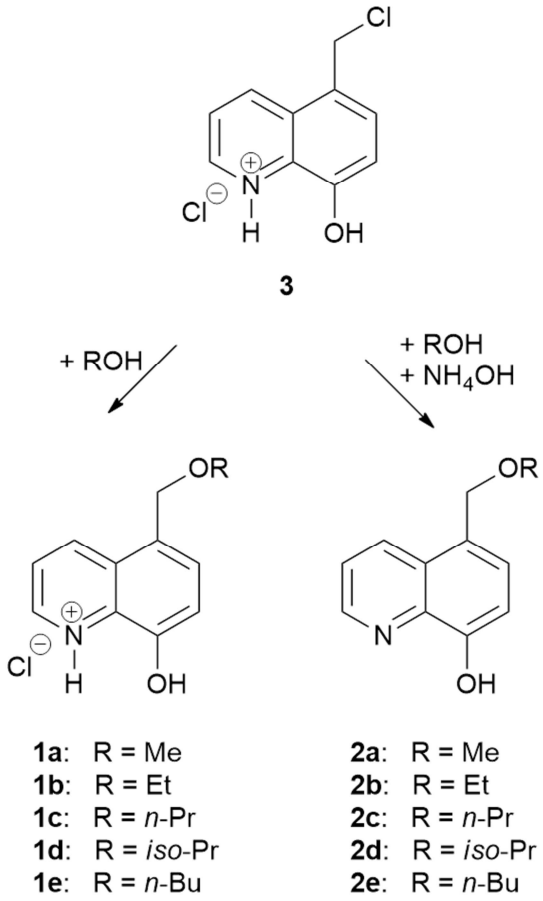

Scheme 1 Synthesis of studied 8-hydroxyquinoline derivatives.

2. Materials and methods

2.1. General

The melting points (uncorrected) were measured on a hot stage microscope (Büchi 510). The IR spectra were recorded on a Perkin Elmer FT-IR 1600 spectrometer as KBr pellet. ^{1}H and ^{13}C NMR spectra were measured on a Bruker Avance III-500 MHz spectrometer using Me_4Si as internal standard. The ESI mass spectra (**1a-1e**) were obtained using a Bruker amazon SL coupled with a Dionex Ultimate 3000 (Thermo Scientific) using a C18 reversed column [3 µm, 120 Å, 2.1 x 100 mm (Acclaim™ from Thermo Scientific)]. The EI mass spectra (**2a-2e**) were recorded on a Perkin Elmer Clarus SQ8S. Elemental analyses were performed on an Elementar CHN VarioMicro Cube analyser.

Starting materials are commercially available. 5-Chloromethyl-8-hydroxyquinolin-1-ium chloride (**3**) has been synthesized from 8-hydroxyquinoline, formaldehyde (37%), concentrated hydrochloric acid and gaseous HCl as described in the literature.[13,14] M.p.: 281℃ dec. (lit. [14] m.p. 280℃ dec.).

2.2. Synthesis

*General procedure for the synthesis of 5-alkoxymethyl-8-hydroxyquinolin-1-ium chlorides (**1a**-**1e**)*

5-Chloromethyl-8-hydroxyquinolin-1-ium chloride (**3**, 2.2 mmol) was dissolved in the corresponding alcohol (30 mL) and heated under reflux for three hours and cooled down to room temperature. Yellow crystals being formed after two weeks at room temperature were washed with the respective alcohol to yield the pure compounds. Specific details for each compound are given below.

*5-Methoxymethyl-8-hydroxyquinolin-1-ium chloride (**1a**).* 5-Chloromethyl-8-hydroxyquinolin-1-ium chloride (**3**, 0.5 g, 2.2 mmol) and methanol (30 mL) were used. Yield 0.41 g (82%); mp: 260℃ (dec.). Anal. Calcd. for $C_{11}H_{12}ClNO_2$: C, 58.54; H 5.36; N, 6.21 %; found: C, 58.06, H, 5.40; N, 6.15 %. IR (KBr): 3000 ν(O-H), 2020 ν(=NH^+-), 1595 ν(C=C_{Ar}), 1548 ν(C=C), 764 δ(C-H) cm^{-1}. ^{1}H NMR (MeOD-d_4): δ_H 9.98 (dd, ^3J = 8.7, 1.4 Hz, 1H, Ar-H), 9.10 (dd, ^3J = 5.3, 1.4 Hz, 1H, Ar-H), 8.16 (dd, ^3J = 8.7, 5.4 Hz, 1H, Ar-H), 7.81 (d, ^3J = 7.9 Hz, 1H, Ar-H), 7.44 (d, ^3J = 7.9 Hz, 1H, Ar-H), 4.92 (s, 2H, Ar-CH_2-O), 3.45 (s, 3H, O-CH_3) ppm; ^{13}C NMR (MeOD-d_4) δ_C 148.1 (C-8), 144.4 (C-1), 142.8 (C-9), 131.4 (C-3), 129.6 (C-6), 129.0 (C-5), 126.1 (C-4), 121.9 (C-2), 114.9 (C-7), 71.1 (C-10), 57.0 (C-11) ppm. MS (ESI) m/z: found – 189.80 $[M]^+$; calc. for $C_{11}H_{12}NO_2^+$ – 190.09.

*5-Ethoxymethyl-8-hydroxyquinolin-1-ium chloride (**1b**).* 5-Chloromethyl-8-hydroxyquinolin-1-ium chloride (**3**, 0.5 g, 2.2 mmol) and ethanol (30 mL) were used. Yield 0.45 g (86%); mp: 207 ℃. Anal. Calcd. $C_{12}H_{14}ClNO_2$: C, 60.13; H, 5.89; N, 5.84 %; Found: C, 59.88; H, 6.27; N, 5.87 %. IR (KBr): 2908 ν(O-H), 2026 ν(=NH^+-), 1595 ν(C=C_{Ar}), 1550 ν(C=C), 769 δ(C-H) cm^{-1}. ^{1}H NMR (MeOD-d_4): δ_H 9.39 (dd, ^3J = 8.6, 1.4 Hz, 1H, Ar-H), 9.11

(dd, ^{3}J = 5.4, 1.4 Hz, 1H, Ar-H), 8.17 (dd, ^{3}J = 8.6, 5.4 Hz, 1H, Ar-H), 7.80 (d, ^{3}J = 7.9 Hz, 1H, Ar-H), 7.44 (d, ^{3}J = 7.9 Hz, 1H, Ar-H), 4.97 (s, 2H, Ar-CH_2-O), 3.67 (q, ^{3}J = 7.0 Hz, 2H, O-CH_2-CH_3), 1.24 (t, ^{3}J = 7.0 Hz, 3H, O-CH_2-CH_3) ppm.^{13}C NMR (MeOD-d_4) δ_C 148.0 (C-8), 144.4 (C-1), 142.8 (C-9), 131.2 (C-3), 129.5 (C-6), 129.0 (C-5), 126.5 (C-4), 121.9 (C-2), 115.0 (C-7), 69.2 (C-10), 65.6 (C-11), 14.1 (C-12) ppm. MS (ESI) m/z: found – 203.84 $[M]^+$; calc. for $C_{12}H_{14}NO_2^+$ – 204.10.

*5-n-Propoxymethyl-8-hydroxyquinolin-1-ium chloride (**1c**).* 5-Chloromethyl-8-hydroxyquinolin-1-ium chloride (**3**, 0.5 g, 2.2 mmol) and *n*-propanol (30 mL) were used. Yield 0.47 g (85%); mp: 220 ℃. Anal. Calcd. $C_{13}H_{16}ClNO_2$: C, 61.54; H 6.36; N, 5.52 %; Found: C, 61.42; H, 6.56; N, 5.61 %. IR (KBr): 2902 ν(O-H), 2027 ν(=NH^+-), 1596 ν(C=C_{Ar}), 1549 ν(C=C), 766 δ(C-H) cm^{-1}. ^{1}H NMR (MeOD-d_4): δ_H 9.40 (dd, ^{3}J = 8.7, 1.4 Hz, 1H, Ar-H), 9.09 (dd, ^{3}J = 5.3, 1.4 Hz, 1H, Ar-H), 8.16 (dd, ^{3}J = 8.7, 5.4 Hz, 1H, Ar-H), 7.82 (d, ^{3}J = 7.9 Hz, 1H, Ar-H), 7.45 (d, ^{3}J = 7.9 Hz, 1H, Ar-H), 4.98 (s, 2H, Ar-CH_2-O), 3.56 (t, ^{3}J = 6.5 Hz, 2H, O-CH_2-CH_2-CH_3), 1.70 – 1.59 (m, 2H, O-CH_2-CH_2-CH_3), 0.93 (t, ^{3}J = 7.4, 3H, O-CH_2-CH_2-CH_3) ppm. ^{13}C NMR (MeOD-d_4) δ_C 148.1 (C-8), 144.4 (C-1), 142.8 (C-9), 131.2 (C-3), 129.7 (C-6), 129.1 (C-5), 126.6 (C-4), 121.8 (C-2), 114.9 (C-7), 71.9 (C-10), 69.4 (C-11), 22.5 (C-12), 9.6 (C-13) ppm. MS (ESI) m/z: found 217.84 $[M]^+$; calc. for $C_{13}H_{16}NO_2^+$ – 218.12.

*5-iso-Propoxymethyl-8-hydroxyquinolin-1-ium chloride (**1d**).* 5-Chloromethyl-8-hydroxyquinolin-1-ium chloride (**3**, 0.5 g, 2.2 mmol) and *iso*-propanol (30 mL) were used. Yield 0.40 g (72%); mp: 161 ℃. Anal. Calcd. $C_{13}H_{16}ClNO_2$: C, 61.54; H 6.36; N, 5.52 %; Found: C, 61.31; H, 6.49; N, 5.64 %. IR (KBr): 2964 ν(O-H), 2028 ν(=NH^+-), 1597 ν(C=C_{Ar}), 1551 ν(C=C), 766 δ(C-H) cm^{-1}. ^{1}H NMR (MeOD-d_4): δ_H 9.39 (dd, ^{3}J = 8.6 Hz, 1.4, 1H, Ar-H), 9.10 (dd, ^{3}J = 5.4 Hz, 1.4, 1H, Ar-H), 8.17 (dd, ^{3}J = 8.7, 5.3 Hz, 1H, Ar-H), 7.82 (d, ^{3}J = 8.0 Hz, 1H, Ar-H), 7.44 (d, ^{3}J = 7.9 Hz, 1H, Ar-H), 4.99 (s, 2H, Ar-CH_2-O), 3.86 (m, 1H, O-CH-$(CH_3)_2$), 1.25 (d, ^{3}J = 6.1 Hz, 6H, CH-$(CH_3)_2$) ppm. ^{13}C NMR (MeOD-d_4) δ_C 148.0 (C-8), 144.4 (C-1), 142.7 (C-9), 131.0 (C-3), 129.6 (C-6), 129.1 (C-5), 126.9 (C-4), 121.8 (C-2), 115.0 (C-7), 71.5 (C-10), 66.8 (C-11), 21.0 (C-12, C-13) ppm. MS (ESI) m/z: found – 217.86 $[M]^+$; calc. for $C_{13}H_{16}NO_2^+$ – 218.12.

*5-n-Butoxymethyl-8-hydroxyquinolin-1-ium chloride (**1e**).* 5-Chloromethyl-8-hydroxyquinolin-1-ium chloride (**3**, 0.5 g, 2.2 mmol) and *n*-butanol (30 mL) were used. Yield 0.32 g (55 %); mp: 171 ℃. Anal. Calcd. $C_{14}H_{18}ClNO_2$: C, 62.80; H 6.78; N, 5.23 %; Found: C, 62.73; H, 6.98; N, 5.14 %. IR (KBr): 2952 ν(O-H), 2051 ν(=NH^+-), 1594 ν(C=C_{Ar}), 1548 ν(C=C), 772 δ(C-H) cm^{-1}. ^{1}H NMR (MeOD-d_4): δ_H 9.38 (dd, ^{3}J = 8.7, 1.4 Hz, 1H, Ar-H), 9.12 (dd, ^{3}J = 5.3, 1.4 Hz, 1H, Ar-H), 8.18 (dd, ^{3}J = 8.7, 5.4 Hz, 1H, Ar-H), 7.79 (d, ^{3}J = 7.9 Hz, 1H, Ar-H), 7.44 (d, ^{3}J = 7.9 Hz, 1H, Ar-H), 4.95 (s, 2H, Ar-CH_2-O), 3.59 (t, ^{3}J = 6.5 Hz, 2H, O-CH_2-CH_2-CH_2-CH_3), 1.58 – 1.61 (m, 2H, O-CH_2-CH_2-CH_2-CH_3), 1.35 – 1.40 (m, 2H, O-CH_2-CH_2-CH_2-CH_3), 0.90 (t, ^{3}J = 7.4, 3H, O-CH_2-CH_2-CH_2-CH_3) ppm. ^{13}C NMR (MeOD-d_4) δ_C 148.0 (C-8), 144.4 (C-1), 142.8 (C-9), 131.2 (C-4), 129.5 (C-6), 129.0 (C-5), 126.5 (C-4), 121.9 (C-2), 115.0 (C-7), 70.0 (C-10), 69.4 (C-11), 31.5 (C-12), 19.0 (C-13), 12.8 (C-14) ppm. MS (ESI) m/z: found 232.08 $[M]^+$; calc. for $C_{14}H_{18}NO_2^+$ – 232.13.

*General procedure for the synthesis of 5-alkoxymethyl-8-hydroxyquinolines (**2a**-**2e**).*

5-Chloromethyl-8-hydroxyquinolin-1-ium chloride (**3**, 4.4 mmol) was dissolved in the corresponding alcohol (30 mL) and heated under reflux. The alcohol was distilled off under reduced pressure and the residue suspended in diethyl ether (10 mL). An aqueous ammonia solution (2.5 %) was added dropwise until the solid is dissolved. The organic phase was washed two times with water (à 5 mL), dried over Na_2SO_4 and evaporated slowly. Specific details for each compound are given below.

*5-Methoxymethyl-8-hydroxyquinoline (**2a**).* 5-Chloromethyl-8-hydroxyquinolin-1-ium chloride (**3**, 0.5 g, 2.2 mmol) and methanol (30 mL) were used. Yield 0.35 g (42%); mp: 81.2 ℃, lit. [15,16] mp: 79-80 and 83℃, respectively.

*5-Ethoxymethyl-8-hydroxyquinoline (**2b**).* 5-Chloromethyl-8-hydroxyquinolin-1-ium chloride (**3**, 0.5 g, 2.2 mmol) and ethanol (30 mL) were used. Yield 0.48 g (54%); mp: 84 ℃, lit.[14] mp: 83-83.5 ℃. Anal. Calcd. $C_{12}H_{13}NO_2$: C, 70.92; H, 6.45; N, 6.89 %; Found: C, 70.74, H, 6.80; N, 6.87 %. IR (KBr): 3314 ν(O-H), 2973 ν(-CH_3), 2862 ν(-CH_2-), 1578 ν(C-O_{OH}), 1506 ν(C=C_{Ar}), 793 δ(C-H) cm^{-1}. ^{1}H NMR ($CDCl_3$) δ_H 8.76 (dd, ^{3}J = 4.3, 1.6 Hz, 1H, Ar-H),

8.46 (dd, ^{3}J = 8.5, 1.6 Hz, 1H, Ar-H), 7.43 (dd, ^{3}J = 8.5, 4.2 Hz, 1H, Ar-H), 7.38 (d, ^{3}J = 7.7 Hz, 1H, Ar-H), 7.10 (d, ^{3}J = 7.7 Hz, 1H, Ar-H), 4.79 (s, 2H, Ar-CH_2-O), 3.55 (q, ^{3}J = 7.0 Hz, 2H, O-CH_2-CH_3), 1.21 (t, ^{3}J = 7.0 Hz, 3H, O-CH_2-CH_3) ppm.^{13}C NMR ($CDCl_3$) δ_C 152.5 (C-8), 147.7 (C-1), 138.7 (C-5), 133.5 (C-9), 128.7 (C-3), 127.5 (C-4), 124.7 (C-6), 121.8 (C-2), 109.0 (C-7), 70.7 (C-10), 65.5 (C-11), 15.3 (C-12) ppm. MS (EI) m/z: found – 203 $[M]^{+\cdot}$; 158 (100), calc. for $C_{12}H_{13}NO_2$ – 203.09.

*5-n-Propoxymethyl-8-hydroxyquinoline (**2c**).* 5-Chloromethyl-8-hydroxyquinolin-1-ium chloride (**3**, 0.5 g, 2.2 mmol) and *n*-propanol (30 mL) were used. Yield 0.70 g (74%); mp: 78 ℃, lit.[15] mp: 76-77 ℃. Anal. Calcd. $C_{13}H_{15}NO_2$: C, 71.87; H, 6.96; N, 6.45 %; Found: C, 72.19, H, 7.23; N, 6.49 %. IR (KBr): 3294 ν(O-H), 2968 ν(-CH_3), 2862 ν(-CH_2-), 1579 ν(C-O_{OH}), 1505 ν(C=C_{Ar}), 785 δ(C-H) cm^{-1}. ^{1}H NMR ($CDCl_3$) δ_H 8.77 (dd, ^{3}J = 4.1, 1.5 Hz, 1H, Ar-H), 8.46 (dd, ^{3}J = 8.5, 1.6 Hz, 1H, Ar-H), 7.44 (dd, ^{3}J = 8.5, 4.2 Hz, 1H, Ar-H), 7.42 (s, 1H, Ar-H), 7.09 (d, ^{3}J = 7.7 Hz, 1H, Ar-H), 4.79 (s, 2H, Ar-CH_2-O), 3.47 (t, ^{3}J = 6.6 Hz, 2H, O-CH_2-CH_2-CH_3), 1.60 (dt, ^{3}J = 14.2, 7.1 Hz, 2H, O-CH_2-CH_2-CH_3), 0.88 (t, ^{3}J = 7.4, 3H, O-CH_2-CH_2-CH_3) ppm. ^{13}C NMR ($CDCl_3$) δ_C 152.5 (C-8), 147.7 (C-1), 138.7 (C-5), 133.6 (C-9), 128.6 (C-3), 127.5 (C-4), 124.8 (C-6), 121.8 (C-2), 109.0 (C-7), 71.8 (C-10), 70.9 (C-11), 23.0 (C-12), 10.7 (C-13) ppm. MS (EI) m/z: found –217 $[M]^{+\cdot}$; 158(100), calc. for $C_{13}H_{15}NO_2$ – 217.11.

*5-iso-Propoxymethyl-8-hydroxyquinoline (**2d**).* 5-Chloromethyl-8-hydroxyquinolin-1-ium chloride (**3**, 0.5 g, 2.2 mmol) and *iso*-propanol (30 mL) were used. Yield 0.51 g (54%); mp: 65 ℃, lit.[14] mp: 65-66 ℃.

*5-n-Butoxymethyl-8-hydroxyquinoline (**2e**).* 5-Chloromethyl-8-hydroxyquinolin-1-ium chloride (**3**, 0.5 g, 2.2 mmol) and *n*-propanol (30 mL) were used. Yield 0.82 g (82%); mp: 49 ℃, lit.[14] mp: 46-47.2 ℃. Anal. Calcd. $C_{14}H_{17}NO_2$: C, 72.70; H, 7.41; N, 6.06 %; Found: C, 72.28; H, 7.83; N, 6.07 %. IR (KBr): 3322 ν(O-H), 2963 ν(-CH_3), 2857 ν(-CH_2-), 1581 ν(C-O_{OH}), 1509 ν(C=C_{Ar}), 784 δ(C-H) cm^{-1}. ^{1}H NMR ($CDCl_3$) δ_H 8.89 (dd, ^{3}J = 4.2, 1.5 Hz, 1H, Ar-H), 8.48 (dd, ^{3}J = 8.5, 1.6 Hz, 1H, Ar-H), 7.45 (dd, ^{3}J = 8.5, 4.2 Hz, 1H, Ar-H), 7.40 (d, ^{3}J = 7.7 Hz, 1H, Ar-H), 7.10 (d, ^{3}J = 7.7 Hz, 1H, Ar-H), 4.80 (s, 2H, Ar-CH_2-O), 3.48 (t, ^{3}J = 6.6 Hz, 2H, O-CH_2-CH_2-CH_2-CH_3), 1.62 – 1.48 (m, 2H, O-CH_2-CH_2-CH_2-CH_3), 1.42 – 1.29 (m,

2H, O-CH_2-CH_2-C<u>H_2</u>-CH_3), 0.90 (t, ^3J = 7.4 Hz, 4H, O-CH_2-CH_2-CH_2-C<u>H_3</u>) ppm. ^{13}C NMR ($CDCl_3$) δ_C 152.4 (C-8), 147.7 (C-1), 138.7 (C-5), 133.6 (C-9), 128.6 (C-3), 127.5 (C-4), 124.8 (C-6), 121.8 (C-2), 108.9 (C-7), 70.9 (C-10), 69.9 (C-11), 31.8 (C-12), 19.4 (C-13), 13.9 (C-14) ppm. MS (EI) m/z: found – 231 $[M]^{+\cdot}$, 158(100), calc. for $C_{14}H_{17}NO_2$ – 231.13.

2.3. Crystal preparation and single crystal structure determination

Single crystals of 5-alkoxymethyl substituted 8-hydroxyquinolin-1-ium chlorides **1a**-**1d** suitable for single crystal X-ray diffraction experiments were grown directly from a hot solution of 5-chloromethyl-8-hydroxyquinolin-1-ium chloride (**3**) in the appropriate alcohol at room temperature. The neutral 5-alkoxymethyl-8-hydroxyquinolines **2a**-**2e** were crystallised from a saturated solution in diethyl ether at room temperature.

Data collection was performed on a STOE IPDS-2T (**1a**, **2a**) or STOE IPDS-2 (**2d**) diffractometer (image plate) equipped with a low-temperature device with Mo-K_α radiation (λ = 0.71073 Å) using ω and φ scans. Software for data collection: X-AREA, cell refinement: X-AREA and data reduction: X-RED.[17] Intensity data collection was also performed on a Bruker Kappa Apex II (**1b**-**1d**, **2b**, **2c** and **2e**) equipped with a low-temperature device with Mo-K_α radiation (λ = 0.71073 Å) using ω and φ scans. Software for data collection and cell refinement: SMART and data reduction: SAINT.[18] Reflections were corrected for background, Lorentzian and polarisation effects. Preliminary structure models were derived by direct methods[19] and the structures were refined by full-matrix least-squares calculations based on F^2 for all reflections using SHELXL.[20] The NH and OH hydrogen atoms of all crystal structures **1a-1d**, and **2a-2e** were located in the difference Fourier map and refined freely. The remaining hydrogen atoms were included in the models in calculated positions and were refined as constrained to the bonding atoms. As shown in Fig. 1, the ethyl group of the structure **1b** is disordered in two positions (54:46). In the crystal structure of **1d**, the rest electron density could not be assigned to a specific solvent molecule. Therefore, the data were refined using SQUEEZE.[21] As a result, two voids were found in the crystal structure with 81 electrons indicating several *iso*-propanol and water molecules. Crystal data are

summarised in the supplementary material. CCDC 1473551-1473559 contain the supplementary crystallographic data for this paper. These data can be obtained free of charge via http://www.ccdc.cam.ac.uk/conts/retrieving.html (or from the Cambridge Crystallographic Data Centre, 12, Union Road, Cambridge CB2 1EZ, UK; fax: +44 1223 336033).

2.4. Hirshfeld analysis

Hirshfeld surfaces[22] and the associated 2D-fingerprint plots[23] were generated for the whole series of crystal structures **1a-1d** and **2a-2e** by means of CrystalExplorer 3.1.[24] But here, only the species **1a** and **2a** are discussed exemplarily in detail including fingerprint plots, d_n surfaces, shape index and curvedness,[25] while the supplementary material contains the corresponding data for **1b-1d** and **2b-e** (Fig. S1 and Fig. S2, respectively). It is noteworthy that the crystal structure of **1d** contains electron density not assigned to a specific solvent molecule. Therefore, the SQUEEZE[21] treatment causes a structure of **1d** with two voids. These voids are shown up in the fingerprint plots of **1d** with a large number of points at high d_i and d_e values.[26,27] 3D d_{norm} surfaces are mapped over a fixed colour scale of −0.3 au (red) - 1.0 Å au (blue). Shape index is mapped in the colour range of −1.0 au (concave) – 1.0 au (convex) Å, and curvedness in the range of −4.0 au (flat) – 0.01 au (singular) Å. The 2D fingerprint plots are displayed by using the translated 0.4 - 3.0 Å range including reciprocal contacts.

2.5. DFT calculations

The quantum chemical calculations were carried out using the GAUSSIAN 09 series of programs.[28] The molecule geometries in Table S1 (supporting information) have been optimized with B3LYP/6-311+G(d,p)[29,30,31,32] in order to obtain information about the preferred conformations of the OH-group in 8-hydroxyquinoline and its protonated derivative. The calculation of Hessian-matrices verified the presence of local minima on the potential energy surface with zero imaginary frequencies for both conformers of **8-HQ** and protonated **8-HQ$^+$**

with H outside (see also column "i" in Table S1). Protonated **8-HQ$^+$** with H inside has one imaginary frequency and represents a transition state on the potential energy surface of this molecule.

Covalent X-H bonds from X-ray structural data are notoriously too short.[33] Thus, different correction methods have been proposed.[34,35,36] The effective X-H distances are crucial for the correct analysis of the electron density distribution around these hydrogen atoms. Therefore, the H atom positions in **1a** and **2a** have been optimized while all other atoms were kept fixed on the positions obtained from the X-ray structural data (Table S2). This partial geometry optimization and the subsequent QTAIM analyses have been performed at the B3LYP/6-311+G(d,p) level. The wave function files for the QTAIM analysis were generated in Cartesian coordinates with a basis set containing 6d functions (option "6D 10F" in Gaussian 09). The electron density topology was analysed using the programs AIM2000[37] and Xaim.[38] Graphical representations for the Laplacian of electron density and electron density of the hydrogen bridged regions of the dimers are shown in the supporting information (Fig. S3 and Fig. S4).

3. Results and discussion

3.1. Synthesis

The 5-alkoxymethyl-8-hydroxyquinoline hydrochlorides **1a**-**1e** were synthesised from 5-chloromethyl-8-hydroxyquinolin-1-ium chloride (**3**) and corresponding alcohols to yield the products as yellow crystals. For preparation of the 5-alkoxymethyl-8-hydroxyquinolines **2a**-**2e**, solutions of the intermediate hydrochlorides **1a**-**1e** were neutralised with aqueous ammonia leading to the isolation of the products as white crystals (Scheme 1).

3.2. Crystal structure description

The asymmetric parts of the unit cell of the hydrochlorides **1a**-**1d** contain one independent molecule (Fig. 1). Except for **1d**, all compounds were found to crystallise without the presence of solvent molecules. However, in **1d** the electron density could not be

assigned to a specific solvent molecule (for details see Experimental section). All bond angles and lengths of the molecules are in the range of expected values[39] and the aromatic moiety is nearly planar as indicated by the r.m.s of 0.017 in average.

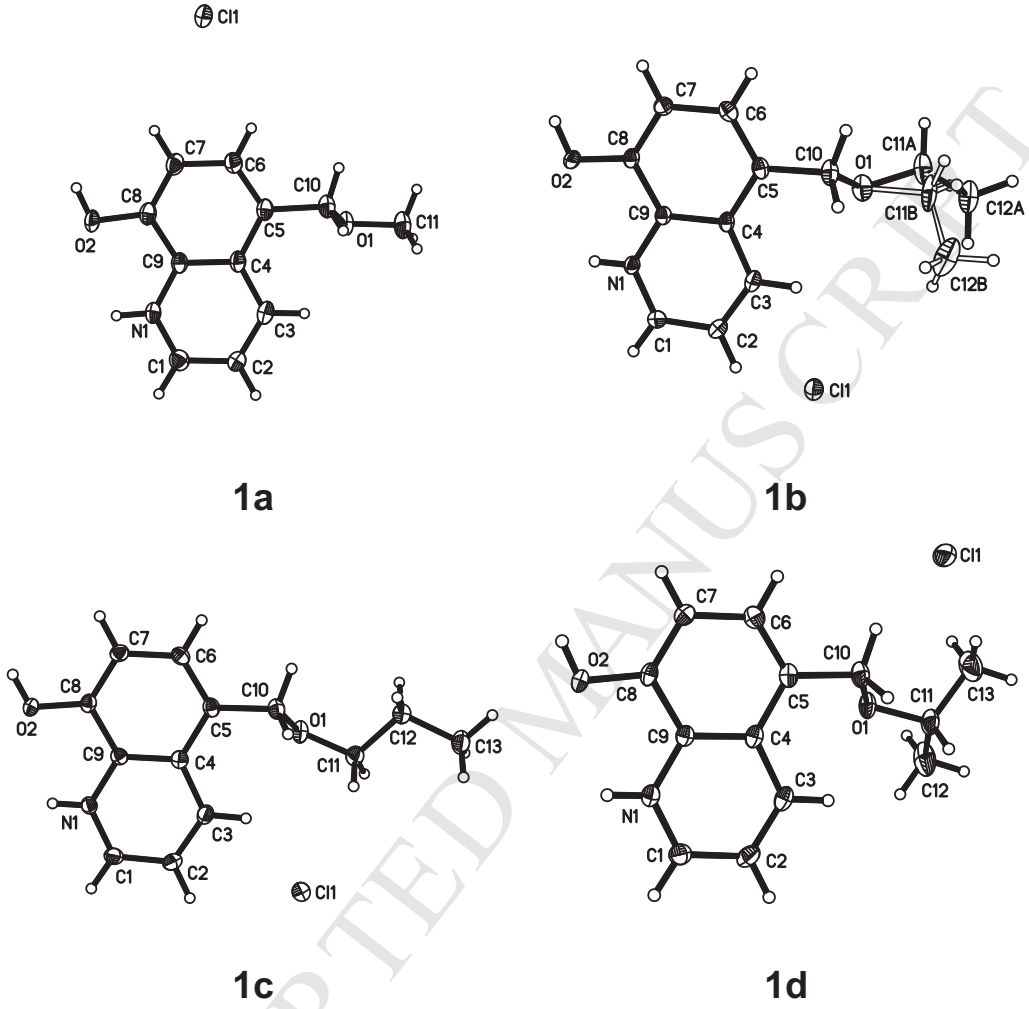

Fig. 1 Molecular structures of **1a**-**1d** showing the atom labelling scheme and displacement ellipsoids drawn at the probability level of 50%. The ethyl group of compound **1b** is disordered in two positions (54:46).

Hence, the molecular geometries of the compounds **1a-1d** are closely comparable to one another differing only in the orientation of the side chain (Fig. 1). In **1a**-**1d**, the oxygen atom of the chain points to the same direction (torsion angles C6/C4-C5-C10-O1 in Table 1). In contrast, the alkyl group bonded at the oxygen atom can exhibit several orientations as obvious from the torsion angle C11-O1-C10-C5. The respective torsion angles are

about -168° in average in **1a**, **1c** and **1d**. The ethoxy substituted derivative **1b** reveals a disorder of the ethyl moiety resulting in two orientations (154° and -179°).

Table 1. Selected torsion angles of compounds **1a-1d** in deg.

	C4-C5-C10-O1	*C6-C5-C10-O1*	*C11-O1-C10-C5*
1a	69.9(3)	-114.9(3)	-174.7(2)
1b	67.24(21)	-116.18(18)	153.9(3) / -179.1(4)
1c	62.95(15)	-120.93(13)	-155.78(11)
1d	60.66(16)	-123.43(14)	-163.42(12)

In all crystal structures of the N-protonated quinoline derivatives **1a**-**1d**, the hydrogen atom of the hydroxyl group was clearly visible in the difference electron-density maps and found to be turned away from the heterocyclic nitrogen atom (Fig. 1). This hydrogen atom (H1N) is involved in a hydrogen bond with the chlorine atom Cl1. Furthermore, the chlorine interacts with the hydroxyl group resulting in a cyclic pattern of hydrogen bonds to stabilize a dimer (Fig. 2). A similar pattern is described for the unsubstituted parent compound with either chloride,[40] nitrate[41] or triflate[42] as counter ion. The latter species contain additional water molecules not influencing the dimer formation. In contrast, using hydrogen sulfate[43] as counter ion or regarding the hydrochloride derivative in the presence of water[44] show a changed dimer formation. The addition of water to the hydrochloride dimer increases the ring size and gives an additional small ring containing two water molecules and two chlorine atoms. An alternative linear molecular arrangement would require to adopt the protonated hydroxyquinoline a geometry with the OH-group pointing towards the pyridine ring (H inside). This conformation is about 42 kJ/mol higher in energy compared to the conformation with the OH-group directed outside (Table S1). This would be likely a consequence that for protonated hydroxyquinoline derivatives any solid state structure with the OH-group directed towards the pyridine ring moiety is unfavourable.

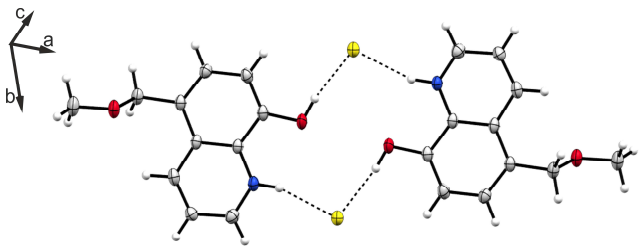

Fig. 2 Dimer formation via N-H···Cl and O-H···Cl hydrogen bonding in the crystal structure of **1a**. Crystal structures of **1b-1d** show an identical hydrogen bonding pattern.

Regarding the described dimers, the average bond length for the O-H···Cl hydrogen bond is 2.13 Å whereas the average distance for N-H···Cl is 2.26 Å, and the corresponding angles (160°/169°) are in the range of hydrogen bonding typical of these modes of interaction (Table 2).[45,46]

Table 2. Geometric parameters of selected intra- and intermolecular hydrogen bonds in **1a**-**1d**.

	D-H···A	Symmetry	D-H in Å	H···A in Å	D···A in Å	D-H···A in deg
1a	N1-H1N···Cl1	-x+3/2,y+1/2,-z+1	0.89(4)	2.22(4)	3.068(2)	160(3)
	O2-H2O···Cl1	x+1/2,-y+1/2,z	0.89(5)	2.12(5)	2.998(2)	169(4)
	C1-H1···O1	-x+1,-y+1,-z	0.95	2.75	3.278(4)	115.7
	C6-H6···Cl1	x,y,z	0.95	2.92	3.592(3)	129.2
	C7-H7···Cl1	x,y,z	0.95	2.99	3.618(3)	125.2
	C10-H10B···O2	x-1,y,z	0.99	2.63	3.279(3)	123.1
	C11-H11B···Cl1	x-1/2,-y+1/2,z-1	0.98	2.70	3.640(3)	160.0
1b	N1-H1N···Cl1	x,y+1,z	0.85(3)	2.26(3)	3.0446(15)	153(2)
	O2-H2O···Cl1	-x+1,-y+1,-z+1	0.90(3)	2.09(3)	2.9925(13)	175(2)
	C1-H1···Cl1	-x+1/2,y+1/2,z	0.95	2.98	3.4652(18)	113.1
	C2-H2···O1	-x+1,y,-z+1/2	0.95	2.57	3.275(2)	131.1
	C6-H6···Cl1	x+1/2,-y+1/2,-z+1	0.95	2.93	3.6208(18)	130.3
	C11A-H11B···Cl1	-x+1,y,-z+1/2	0.99	2.81	3.740(6)	156.7
	C11B-H11D···Cl1	-x+1,y,-z+1/2	0.99	2.92	3.735(7)	140.5
1c	N1-H1N···Cl1	x,y,z+1	0.863(19)	2.26(2)	3.0518(12)	152.4(17)
	O2-H2O···Cl1	-x,-y+1,-z+1	0.86(2)	2.13(2)	2.9866(10)	178(2)
	C3-H3···O1	x,y,z	0.95	2.53	3.0599(17)	115.4
	C10-H10B···O2	-x,-y+1,-z+1	0.99	2.68	3.4543(17)	135.8
	C13-H13A···Cl1	-x+1,-y+1,-z	0.98	2.93	3.8856(16)	165.7
1d	N1-H1N···Cl1	-x+1,-y+1,-z+2	0.858(19)	2.31(2)	3.0880(12)	150.9(17)
	O2-H2O···Cl1	x,y,z+1	0.84(2)	2.17(2)	3.0091(10)	173.9(19)
	C1-H1···Cl1	x+1/2,-y+1,-z+3/2	0.95	2.99	3.4611(14)	112.4

C10-H10B···O2	x,y,z-1	0.99	2.66	3.5220(16)	146.3
C12-H12B···O1	x,-y+1/2,z-1/2	0.98	2.68	3.5697(18)	151.3

Moreover, these centrosymmetric dimers show an offset to one another. While the angle between the planes of the monomer units is zero, the distances (**1a**: 0.699, **1b**: 0.129, **1c**: 0.325, **1d**: 0.366 Å) are significantly shorter than those existing in the protonated parent hydrochloride[40] with a distance of 1.791 Å between adjacent heterocycles.

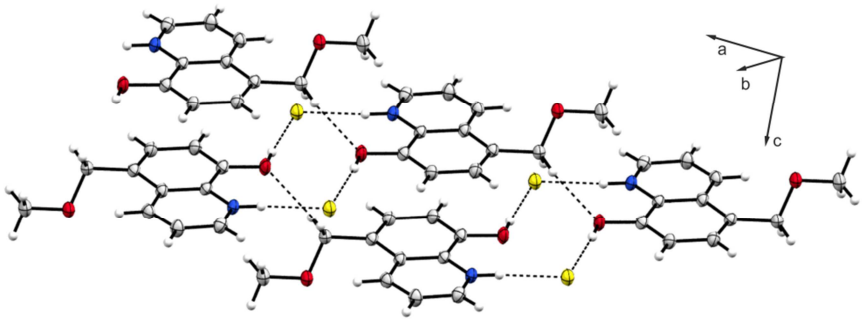

Fig. 3 Molecular packing of **1a** showing C-H···O contacts connecting adjacent dimers created from N-H···Cl and O-H···Cl interactions.

In the molecular packing arrangement of **1a**-**1d**, the dimers are connected via several C-H···O and weak C-H···Cl contacts[47] with aromatic as well as aliphatic hydrogen atoms being involved in these interactions (Table 2). This is especially true for the hydrogen atoms of the alkoxy groups influencing the described orientations of the alkoxy substituent by the interaction. For instance, the CH_2 moiety in **1a** shows an obvious C-H···O contact (Fig. 3.). Apart from one of the disordered ethoxy groups in **1b**, in **1a**-**1d** remarkably no C-H···π contacts occur otherwise being rather frequently observed in solid state structures of aromatic compounds.[48] Instead, π···π stacking interactions[49] of the aromatic units in the range of 3.45 to 3.92 Å are found in the structures leading only in the case of **1a** to molecular strands, while **1b**-**1d** show only molecular π···π stacking dimers.

The unprotonated compounds **2a**-**2d** were found to crystallise with one molecule in the asymmetric part of the unit cell, **2e** crystallises with two independent molecules (Fig. 4). All

heterocyclic moieties in **2a**-**2e** show the expected planarity (r.m.s. of 0.013 in average) and the expected bond lengths and angles.[39]

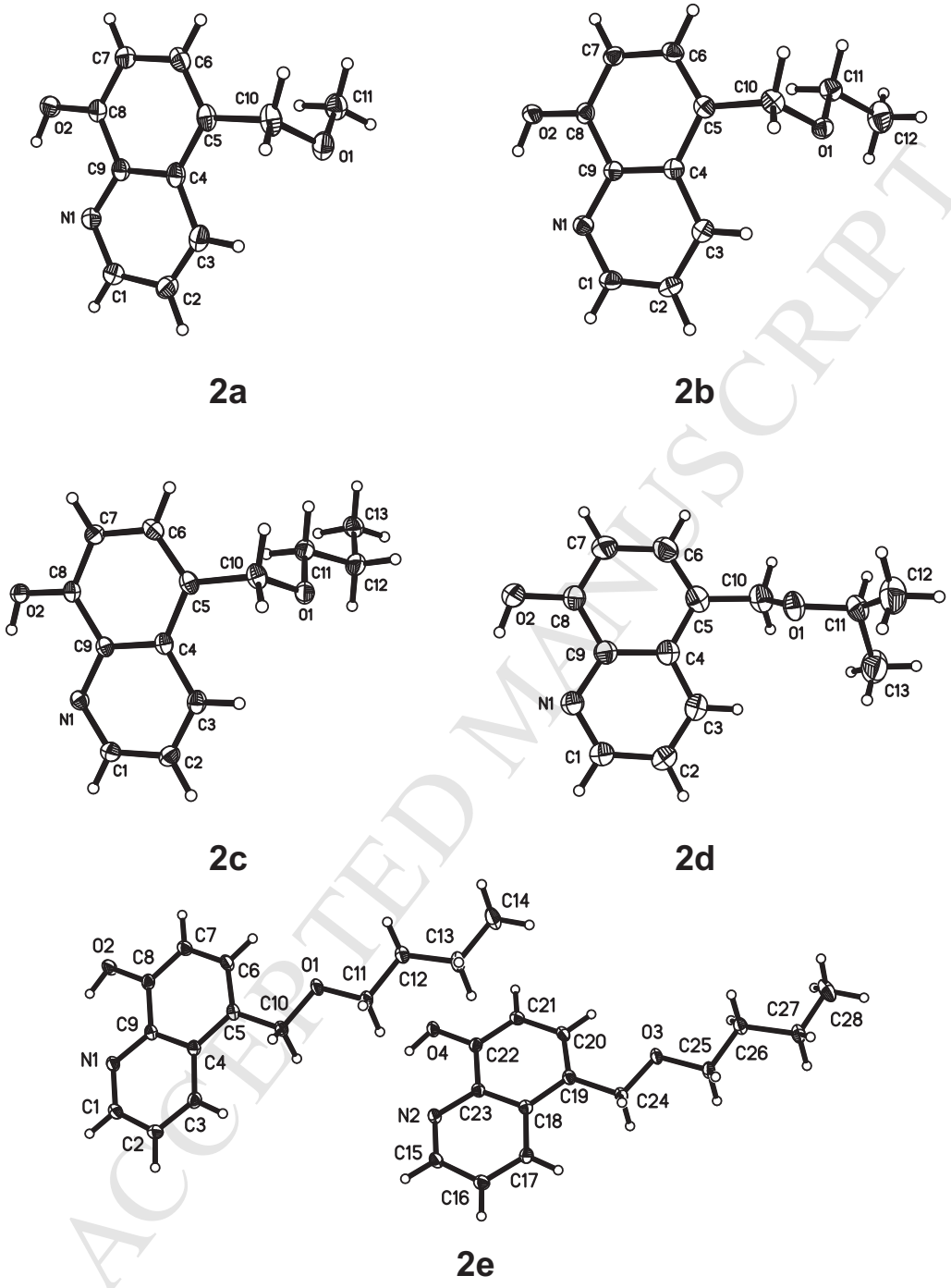

Fig. 4 Molecular structures of **2a**-**2e** showing the atom labelling scheme and displacement ellipsoids drawn at the probability level of 50%.

As observed for the ionic species **1a**-**1d**, the molecular structures of **2a**-**2e** differ in the orientation of their alkoxy substituents. The oxygen atom O1 in **2a**-**2c** points to the opposite

direction compared to **2d** represented in the torsion angle C6-C5-C10-O1 (Table 3). In both molecules of **2e**, the butoxy group is within the plane of the heterocyclic unit (r.m.s. 0.168 and 0.038). Moreover, several orientations of the alkyl group bonded to the oxygen atom are represented in the torsion angle C11-O1-C10-C5 (Table 3). While the smaller representatives featuring methoxy (**2a**), ethoxy (**2b**) and *n*-propoxy (**2c**) groups show a small twist of about 67°, the bulkier quinoline compounds **2d** and **2e** feature an almost planar alkoxy group with torsion angles of nearly 180°.

Table 3. Selected torsion angles of compounds **2a-2e** in deg.

	C4-C5-C10-O1	*C6-C5-C10-O1*	*C11-O1-C10-C5*
2a	66.83(13)	-112.91(11)	64.98(12)
2b	68.72(11)	-110.82(10)	70.18(11)
2c	68.68(12)	-110.10(10)	66.51(11)
2d	-72.58(16)	107.78(15)	177.68(11)
2e	-173.38(9) / -175.15(8)	-6.30(13) / 5.69(13)	-177.62(8) / -176.27(8)

The hydrogen atom of the hydroxyl group was clearly identified in the difference electron-density maps of compounds **2a**-**2e** to form intermolecular hydrogen bonds of the OH···N type with a donor-acceptor distance of about 2.17 Å and a hydrogen acceptor distance of 2.84 Å each on average, respectively (Table 4). This interaction leads to the formation of a dimer similar to the dimer found in the ionic species **1a-1d**, exemplarily illustrated in Fig. 5. The respective hydrogen bonds of **2a-2e** show D-H···A angles between 131 and 136° fitting well into statistical data of interactions between phenolic OH-groups and pyridine nitrogen atoms (Fig. S5).[50] The planar oriented dimers show an offset to one another (**2a**: 0.763, **2b**: 0.526, **2c**: 0.062, **2d**: 0.249 Å). In contrast, the quinoline dimers of the *n*-butoxy derivative **2e** are not planar orientated but show a twist of 19.07°. The unsubstituted and neutral parent compound (8-hydroxyquinoline) is described in two polymorphic forms[51,52,53,54] both showing the same dimer formation as presented here. While form A crystallises in the orthorhombic space group *Fddd* to lead to a non-parallel but twisted (52.8°) quinoline dimer,[52] the monoclinic form B gives a centrosymmetric dimer with a distance of

0.91 Å between adjacent heterocycles.[53] Unlike the described dimers, a linear arrangement of the hydroxyquinoline molecules is reported for the 2,6-dimethyl substituted derivative.[55] The strand requires an outside orientation of the hydroxyl group including a conformation with 32 kJ/mol higher energy (Table S1).

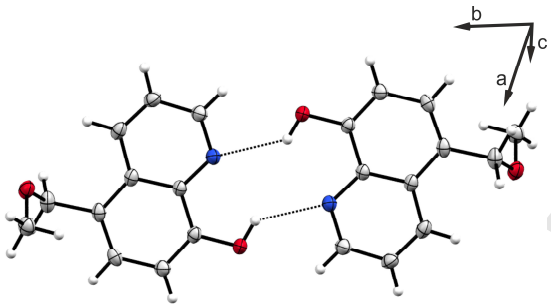

Fig. 5 Dimer formation via N-H···O hydrogen bonding in the crystal structure of **2a**. Crystal structures of **2b-2e** show an identical hydrogen bonding pattern.

The crystal structures of **2a-2e** differ in the arrangement of the dimers caused by intermolecular O-H···N interactions. In the crystal packing of **2a**, no C-H···π contacts are found but on the other hand π···π stacking interactions metrically defined by distances of the centres of gravity of 3.90 and 3.67 Å give rise to molecular strand formation connecting the dimer moieties (Fig. 6a). In addition, several C-H···O contacts stabilise the crystal packing (Table 4). In here, the oxygen atom of the methoxy as well as of the hydroxyl group interacts with hydrogen atoms of the aromatic unit and of the methyl group. The bridging CH_2 group, however, does not show a corresponding interaction in the crystal packing of **2a**.

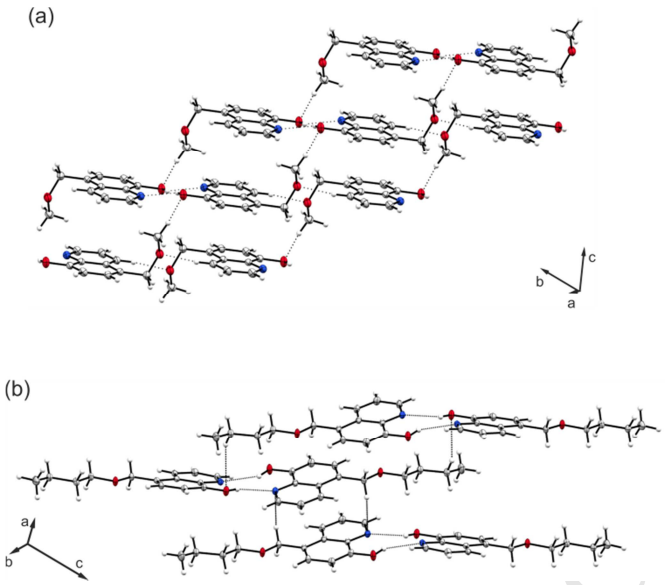

Fig. 6 Molecular packing (a) of **2a** showing π···π and C-H···O interactions and (b) of **2e** showing C-H···π and C-H···O interactions. In both crystal structures the contacts connect adjacent dimers.

Though **2b**-**d** illustrate a conformation similar to **2a**, the interactions occurring in the crystal packing are different in detail. In the packing of **2b**-**d**, C-H···π contacts are becoming more important and in **2d** the stacking interaction is absent. Moreover, in all cases, the aromatic unit does not provide a specific hydrogen atom for hydrogen bonding. Actually, here a CH_2 group being part of the alkyl substituent in **2b**, a methyl group of **2c** or the bridging CH_2 moiety of **2d** interacts via C-H···π contacts to connect adjacent molecules. Therefore, the C-H···π contacts can also be considered as a reason for the orientation of the side chain in the structures of **2a**-**2e**. Especially **2e** which occurs in a complete planar conformation in contrast to **2a**-**2d** comes up with several C-H···π contacts in the range of 2.60 to 2.99 Å (Fig. 6b, Table 4).

Table 4. Geometric parameters of selected intermolecular hydrogen bonds in **2a**-**2e**.

	D-H···A	Symmetry	D-H in Å	H···A in Å	D···A in Å	D-H···A in deg
2a	O2-H2O···N1	-x+1,-y+2,-z	0.860(19)	2.214(18)	2.8603(12)	131.8(14)
	C1-H1···O2	-x+1,-y+2,-z	0.95	2.51	3.0137(14)	113
	C3-H3···O1	-x+1,-y,-z+1	0.95	2.40	3.3044(14)	158.3

2b	O2-H2O···N1	-x+1,-y+1,-z+1	0.865(19)	2.146(19)	2.8286(11)	135.5(15)
	C1-H1···O2	-x+1,-y+1,-z+1	0.95	2.49	3.0026(13)	113.7
	C2-H2···O1	-x+1,y+1/2,-z+1/2	0.95	2.36	3.2514(12)	155.4
	C11-H11A···Cg2[a]	-x+1/2,y-1/2,z	0.99	2.71	3.6492(11)	158.0
2c	O2-H2O···N1	-x,-y+1,-z-1	0.860(18)	2.124(18)	2.7896(11)	134.0(15)
	C1-H1···O2	-x,-y+1,-z-1	0.95	2.47	2.9784(12)	113.8
	C2-H2···O1	-x+1,-y+1,-z	0.95	2.70	3.5081(13)	143.2
	C13-H13A···O1	x,-y+3/2,z-1/2	0.98	2.67	3.5987(13)	158.4
	C13-H13B···O2	x+1,-y+3/2,z+1/2	0.98	2.60	3.4891(13)	150.3
	C13-H13C···Cg1[a]	x,-y+1/2,z-1/2	0.98	2.70	3.8153(12)	166.0
2d	O2-H2O···N1	-x,-y+1,-z+1	0.88(2)	2.21(2)	2.8750(15)	132(2)
	C1-H1···O2	-x,-y+1,-z+1	0.95	2.52	3.0495(17)	115.3
	C2-H2A···O2	x,y-1,z	0.95	2.58	3.4871(18)	159.6
	C10-H10B···O1	x,-y+1/2,z-1/2	0.99	2.63	3.3593(15)	130.6
	C10-H10A···Cg2[a]	x,-y+1/2,z-1/2	0.99	2.84	3.7801(15)	160.0
2e	O2-H2O···N2	-x,-y+1,-z	0.907(18)	2.184(18)	2.8765(11)	132.6(14)
	O4-H4O···N1	-x,-y+1,-z	0.906(19)	2.136(18)	2.8341(11)	133.2(15)
	C1-H1···O4	-x,-y+1,-z	0.95	2.50	3.0032(13)	113.5
	C7-H7···O4	-x,-y,-z	0.95	2.62	3.5376(13)	162.7
	C15-H15···O2	-x,-y+1,-z	0.95	2.58	3.0563(13)	111.5
	C21-H21···O2	-x,-y,-z	0.95	2.61	3.5298(13)	161.9
	C10-H10A···Cg2[a]	-x+1,-y+1,-z	0.99	2.60	3.4924(12)	150.0
	C13-H13B···Cg4[a]	-x+1,-y,-z+1	0.99	2.99	3.9120(12)	155.0
	C25-H25A···Cg4[a]	-x+2,-y,-z+1	0.99	2.69	3.6006(12)	152.0
	C27-H27B···Cg3[a]	-x+1,-y,-z+1	0.99	2.84	3.6572(12)	140

a: Cg is defined as the centroid of the rings (centre of gravity): Cg1: N1,C1-C4,C9; Cg2: C4-C9; Cg3: N2,C15-C18,C23; Cg4: C18-C23.

Observed stacking interactions connect adjacent dimers but do not lead to molecular strands (**2b**: 3.60 Å, **2c**: 3.63 Å, **2e**: 3.77 Å). However, in all the structures of **2a**-**2e**, several C-H···O contacts stabilise the crystal packing including both oxygen atoms (Table 4). Either the methyl group, the CH_2 moiety of the alkyl group or the bridging CH_2 group are involved as hydrogen donor.

3.3. Hirshfeld surface analysis

Hirshfeld surface analysis, especially regarding the fingerprint plots, give quantitative results of the contacts involved in the formation of a crystal packing.[22] Each compound of the two substance classes was subjected to Hirshfeld surface analysis but only results for **1a** and

2a are discussed exemplarily in detail here while corresponding data for **1b**-**1d** and **2b**-**2e**, given in the supporting information (Fig. S1, Fig. S2), are discussed in excerpts.

The fingerprint plot of **1a** presented in Fig. 7a shows two large spikes (1) for the H···Cl/Cl···H contacts to the adjacent molecules. These contacts are obvious in the d_n surface (Fig. 7b) as intense red spots. A cyclic hydrogen bond pattern is usually indicated by a large number of fused spots between the main spikes (1). But here, mainly H···H contacts are shown (3). The small spike indexed with 2 represents H···O contacts. At d_i/d_e values of about 1.8 (red circle) C···C contacts occur.

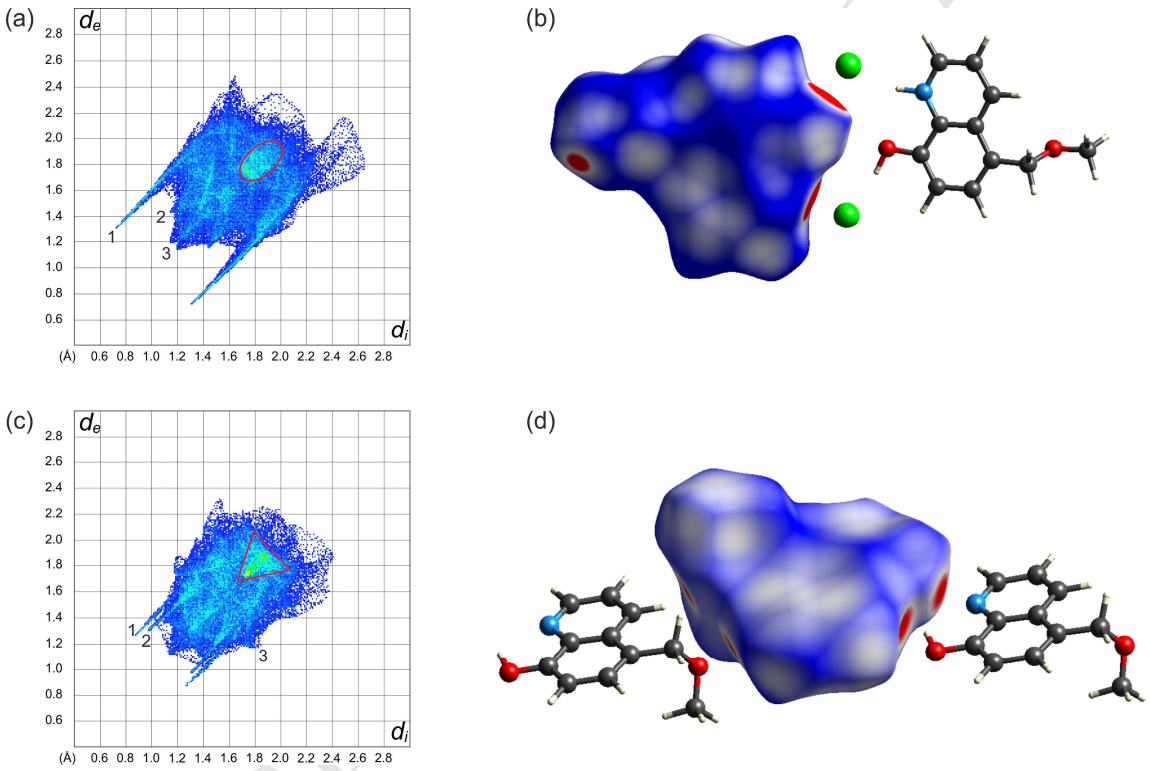

Fig. 7 (a) Fingerprint plot for **1a** with C···C (red circle), H···Cl (1), H···O (2), and H···H (3) contacts, (b) d_{norm} surface for **1a** indicating the H···Cl contacts, (c) fingerprint plot for **2a** with C···C (red triangle), H···N (1), H···O (2), and H···C (3) contacts, (d) d_{norm} surface for **2a** indicating the H···N contacts.

Close C···C contacts mapped with shape index and curvedness from front and back view indicate π···π stacking (Fig. 8). In **1a**, different C···C contacts occur at different sides of the molecule. A flat surface for both rings appears for the front view while the back view

gives only for the N-containing aromatic ring the typical red and blue triangles representative for π···π stacking. The differences being obvious for the two sides and the presence of C···C contacts at both sides prove the molecular strands generated by π···π stacking described above for **1a**.

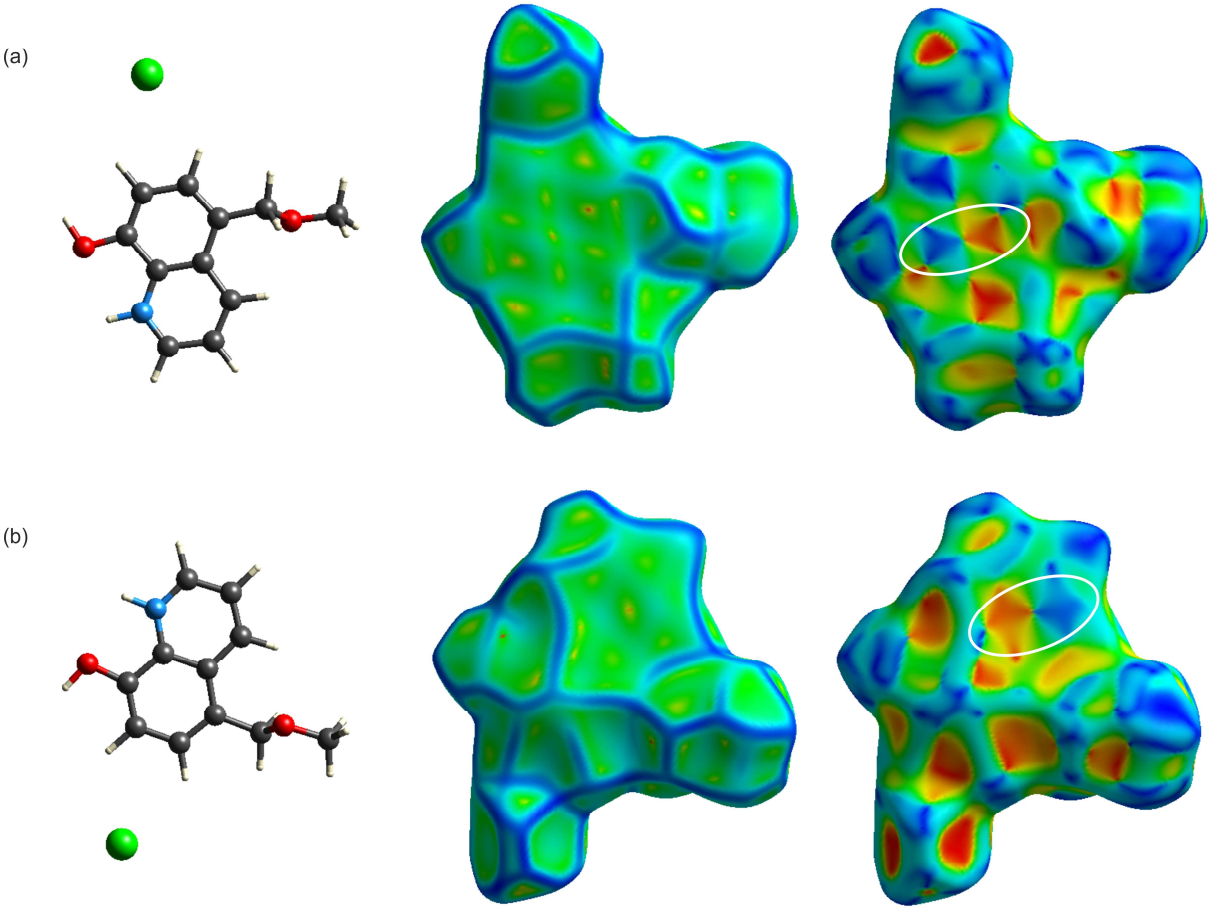

Fig. 8 Hirshfeld surface for **1a**, mapped with shape index (middle) and curvedness (right), (a) front and (b) back view. Highlighted regions on the surfaces are marked with white circles and indicate close C···C contacts.

The methoxy substituted neutral 8-hydroxyquinoline derivative **2a** gives a fingerprint plot as shown in Fig. 7c. At the first sight, the main spikes are less sharp than found for the H···Cl contacts in **1a**. Moreover, H···N contacts (1) occur in addition to the H···O contacts (2). The intense red dots in Fig. 7d indicate the H···N contacts as part of the cyclic hydrogen bond pattern, while the less intense red dots show the H···O contacts of the methoxymethyl group to an adjacent molecule. C···C contacts form a triangle in the fingerprint plot at values

of d_e/d_i of about 1.8. In addition, the curvedness and shape index of both sides of **2a**, depicted in Fig. 9, prove the π···π stacking present in the structure of **2a**. Just as in **1a**, the flat surface appears for both aromatic rings at the front view while the back view shows only C···C contacts for the N-containing ring. In summary, these front and back C···C interactions lead to the formation of molecular strands in the crystal structure of **2a** as described above.

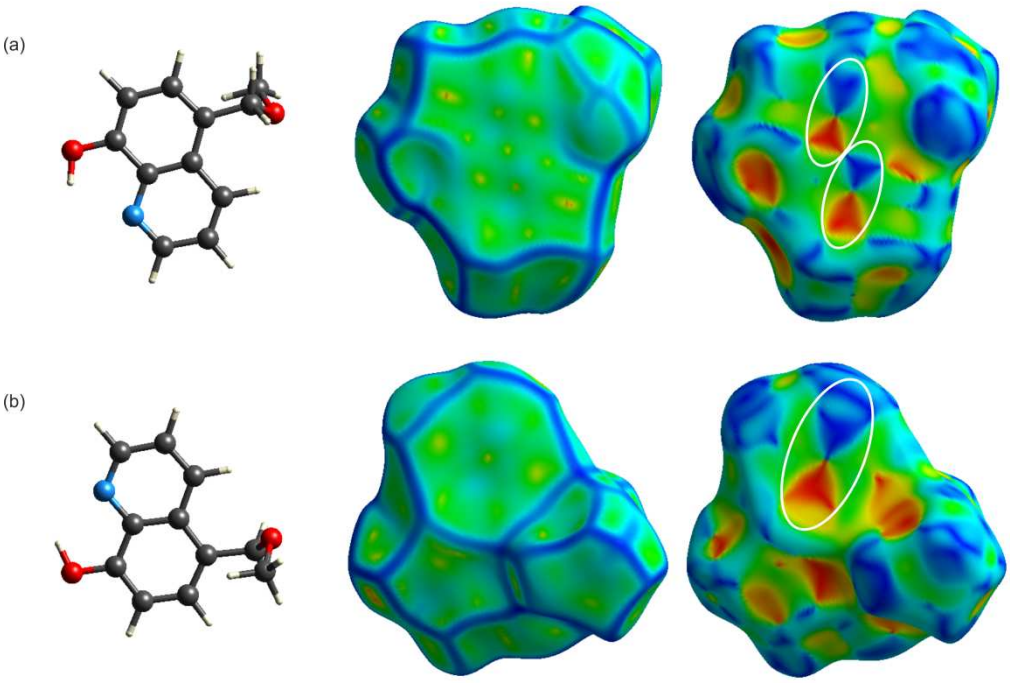

Fig. 9 Hirshfeld surface for **2a**, mapped with shape index (middle) and curvedness (right), (a) front and (b) back view. Highlighted regions on the surfaces are marked with white circles and indicate close C···C contacts.

Fig. 10 shows the distribution of the contacts found in each structure of the protonated hydroxyquinolines **1a-1c** and the neutral molecules **2a-2e**. Apart from the H···H contacts with about 40 to 46%, the crystal structures **1a-1c** are dominated by H···Cl contacts with about 22% followed by H···C (~14%), H···O (~11%) and C···C (5.2%) contacts. Only 1.6% in average of the H···N type of contacts occur (Fig. 10a).

Fig. 10 Relative contribution of the different contacts towards the Hirshfeld surface of the molecules (a) **1a**-**1c** and (b) **2a**-**2e**. The number on the graphs shows the percentage contribution to the Hirshfeld surface by the corresponding intermolecular interactions.

The absence of chloride in **2a-2e** leads to a higher share of all other contacts in a different order than found for **1a-1c**. Actually, the largest share of contacts refers still to H···H contacts but is followed now by H···C with about 17% and H···O contacts with 13%. Again, H···N contacts proportionally play a minor role with only 6.1%. The C···C contacts are similar in share with 5.6%. Remarkably, the C···C contacts do not occur at all in the second molecule of the *n*-butyl substituted derivative (**2e-B**) just as well as other contacts (Fig. 10b).

Trends being noticeable for **2a**-**2e** are: (1) the share of H···H and H···C contacts increases with increasing chain length of the substituents, and (2) the share of H···O contacts decreases from **2a** to **2e**. These facts fit well the alkyl substitution pattern of the presented hydroxyquinoline compounds.

3.4. Theoretical considerations

8-hydroxyquinoline monomers and dimers have already been investigated by means of quantum chemical methods. Amongst others, proton transfer reactions of 8-hydroxyquinoline monomers, dimers,[56] and water adducts,[57] excited state proton transfer reactions and spectroscopic properties[58,59,60] have been studied in detail. By contrast, less is known about the nature of the hydrogen bonds which are present in dimers such as found in the derivatives of **1** and **2**. The topology of the electron density distribution can be analysed using the quantum theory of atoms in molecules (QTAIM) as developed by Bader and others.[61,62,63,64,65] Main features of the topological analysis of the electron density have been described previously.[66] The AIM analysis is an extremely useful tool to understand the bonding situation in a given molecule including the nature of the hydrogen bonds which are involved to neighbouring molecules.[65] According to Rozas *et al.* hydrogen bonds can be classified on the basis of energy and topological data.[67] This classification is based on the properties of the bond critical point (BCP) between the hydrogen atom and the acceptor atom A in hydrogen bonds of type D-H···A. Weak hydrogen bonds have hydrogen bond energies smaller than 50 kJ/mol, a positive Laplacian $\nabla^2\rho$, and a positive electron energy density H. Hydrogen bonds of medium strength have bond energies between 50 and 100 kJ/mol, a positive Laplacian $\nabla^2\rho$, and a negative electron energy density H. Strong hydrogen bonds have bond energies greater than 100 kJ/mol, a negative Laplacian $\nabla^2\rho$, and a negative electron energy density H.[67] This classification shows a continuous transition from weak hydrogen bonds to van der Waals interactions on one side, and on the other side a transition from strong hydrogen bonds to covalent and polar bonds.[68] Espinosa *et al.* have proposed a

proportionality between the hydrogen bond energy E_{HB} and the potential energy density V at the bond critical point: E_{HB} = 0.5 V. [69,] This relation is used below to estimate the hydrogen bond energies. Further information might be drawn from the ratio –V/G at the bond critical point between H and A. The potential energy density V describes the pressure of the hydrogen bonded system on the electrons at the BCP. The kinetic energy density G describes the pressure exerted by those electrons on the hydrogen bonded system.[69, 70] A ratio –V/G < 1 indicates a depletion of electrons at the BCP, which corresponds to a closed shell, or non-covalent interaction. A ratio –V/G > 2 indicates an accumulation of electrons at the BCP. This corresponds to a shared-shell interaction, or in other words a covalent bond. Values of –V/G between one and two describe bonds with partial covalent and partial ionic character.[68,71]

The compounds **1a** and **2a** were chosen as representative derivatives for the class of substances discussed in this paper. The molecular graphs of **1a** and **2a** are shown in Fig. 11. At first sight the bond critical points (BCP) between the atoms of the molecules have the topology as one would describe with a classical Lewis structure.

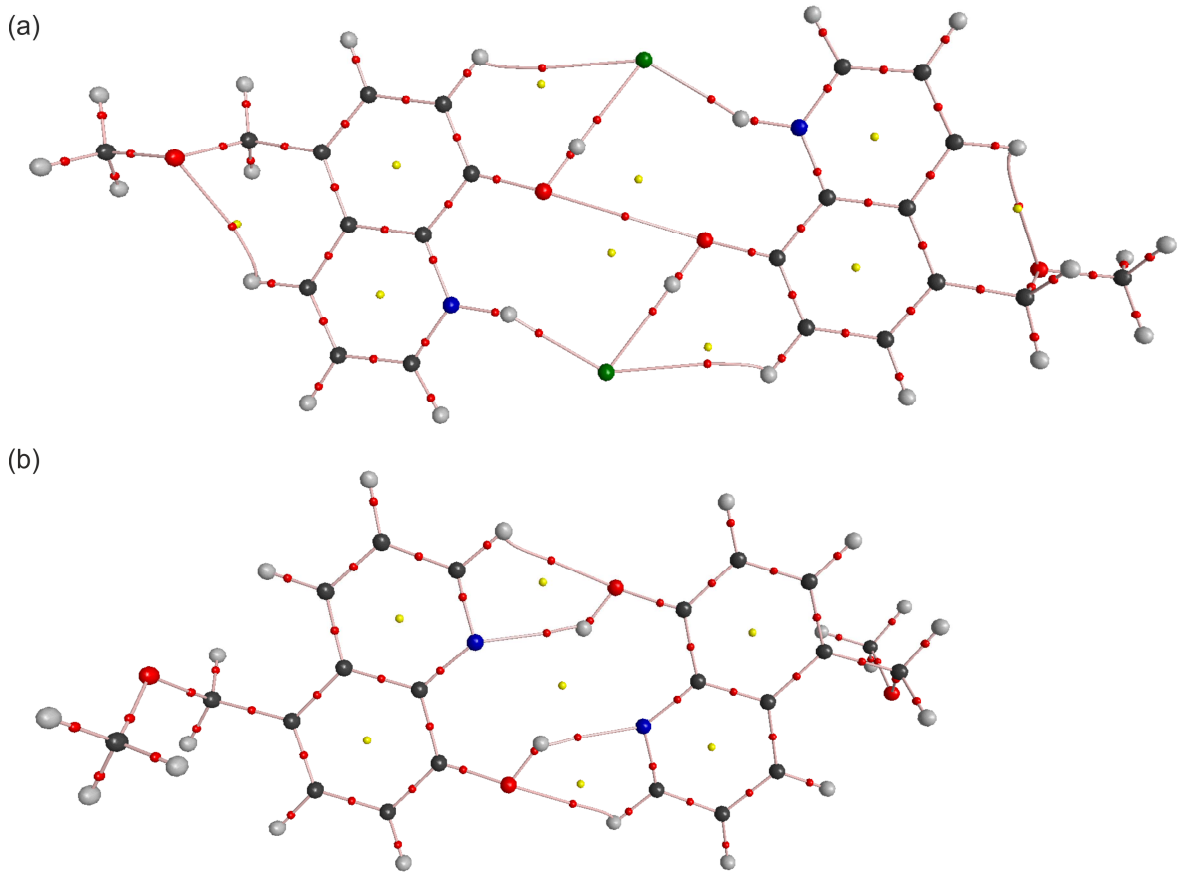

Fig. 11 Molecular graphs of the dimers of (a) **1a** and (b) **2a** with critical points. Bond critical points (BCP) are red, ring critical points yellow, atomic spheres are drawn with arbitrary radii.

Beyond that, bond critical points are found in the molecular graph of **1a** between Cl1···H2O, Cl1···H1N, Cl1···H7, O1···H3, and O2···H2. The latter two bond critical points are somewhat surprising since they were not seen in the X-ray structure. A closer inspection of the bond critical points is possible with the numeric values shown in Table 5. The BCP's between O2-H2O, N1-H1N, and C7-H7 show typical values for covalent bonds: High electron density ρ at the BCP (0.28 to 0.31), negative values for the Laplacian $\nabla^2\rho$, and high values for the ratio –V/G (9 to 11). The BCP's between Cl1···H2O and Cl1···H1N have electron densities at the BCP's which are one order of magnitude smaller than the covalent bonds (0.040 and 0.037). The positive Laplacian $\nabla^2\rho$ is typical for medium and for weak hydrogen bonds. The electron energy density H for both hydrogen bonds have negative values which are very close to zero (-0.007 and -0.005). These values indicate hydrogen bonds with

intermediate character between medium and weak. The hydrogen bond energies E_{HB} of both bonds are below 50 kJ/mol. This indicates that both bonds should be considered as weak interactions. The ratio -V/G is 1.3 and 1.2, respectively. This hints to partial ionic character of this interaction, which might be explained with the negative charge of the chloride ion. The interactions between Cl1···H7, O1···H3, and O2···O2should be characterized as very weak contacts or van der Waals interactions (Table 5). The following arguments are presented for this view: The electron density at the BCP's is one order of magnitude lower than for the hydrogen bonds (0.005 to 0.009). The BCP's of Cl1···H7 and O1···H3 are very close to the corresponding ring critical points in Fig. 11. If the ring critical point and the bond critical point coalesce, they annihilate each other[65] and the interaction between those atoms exists no longer.

Table 5. Electron density ρ, Laplacian $\nabla^2\rho$, potential energy density V, kinetic energy density G, ratio -V/G, electron energy density H (in a.u.), and hydrogen bond energy E_{HB} (in kJ/mol) at selected bond critical points in **1a** and **2a**.

Compound	*Bond*	*ρ*	*∇2ρ*	*G*	*V*	*-V/G*	*H*	E_{HB}
1a	O2-H2O	0.312	-2.118	0.065	-0.659	10.2	-0.594	
	N1-H1N	0.290	-1.518	0.041	-0.462	11.2	-0.421	
	C7-H7	0.284	-0.990	0.035	-0.317	9.2	-0.282	
	Cl1···H2O	0.040	0.070	0.024	-0.031	1.3	-0.007	40.9
	Cl1···H1N	0.037	0.066	0.021	-0.026	1.2	-0.005	33.9
	Cl1···H7	0.006	0.020	0.004	-0.003	0.8	0.001	4.0
	O1···H3	0.009	0.035	0.007	-0.006	0.8	0.001	7.9
	O2···O2	0.005	0.022	0.005	-0.004	0.8	0.001	
2a	O2-H2O	0.346	-2.450	0.064	-0.740	11.6	-0.676	
	C1-H1	0.289	-1.020	0.033	-0.321	9.7	-0.288	
	N1···H2O	0.021	0.071	0.016	-0.014	0.9	0.002	18.5
	O2···H1	0.010	0.042	0.009	-0.007	0.8	0.002	9.2

The bonds between O2-H2O and C1-H1 in the molecular graph of **2a** are classified as covalent bonds with high values of electron density at the BCP's (0.346 and 0.289), negative values of the Laplacian $\nabla^2\rho$, and high values for the ratio –V/G. The intermolecular interactions in the dimer between N1···H2O and O2···H1 have one order of magnitude lower electron density at the BCP's (0.021 and 0.01). These interactions can be classified as weak

hydrogen bonds with a positive Laplacian $\nabla^2\rho$, and a positive electron energy density H. The hydrogen bond energies are 18.5 (N1…H2O) and 9.2 kJ/mol (O2…H1) respectively. This low hydrogen bond energies confirms the presence of weak hydrogen bonds. The ratio -V/G is 0.9 and 0.8, respectively, which indicates a closed shell interaction typical for a hydrogen bond.

4. Comparative Reflections and conclusions

A systematic structural study has been carried out to get knowledge of the packing behaviour and supramolecular interaction modes of a series of differently substituted derivatives of 8-hydroxyquinolines. The data obtained from single crystal X-ray structures, Hirshfeld surface analyses, and quantum chemical calculations permit the following statements: The comparison of the charged quinolines **1a-d** with the neutral quinolines **2a-2e** reveals small differences in the orientation of the side chain for all compounds represented in the torsion angle at the bridging CH_2 group (C10) being either about -110° or 65°, respectively. Furthermore, the side chain is orientated in the same direction, away from the aromatic moiety with the exception of **2d** and **2e**.

The main difference between the neutral and protonated quinolines is the orientation of the hydroxyl H-atom showing outside (**1a-1d**) or inside (**2a-2e**) the cavity. In both cases, the hydroxyl group is involved in intermolecular hydrogen bonds. All crystal structures show a similar hydrogen bond motif which is a cyclic dimer. The insertion of the hydrogen and chlorine atoms into the cyclic dimer found in **1a**-**1d**, leads to the decrease of the ring size. The cyclic dimers feature an offset between adjacent molecules (0.06-0.76 Å, 0.39 Åo n average) in all the crystal structures except for **2e** showing no offset but a torsion of about 19.1°.

In the crystal structures of the charged derivatives **1a-1d** no C-H···π contacts are involved. In contrast, the neutral compounds **2a**-**2e** show C-H···π interactions. The share of these H···C contacts increases depending on the length of the side chain. Furthermore, H···H

contacts increase with the length of side chain while the share of the H···O contacts decreases. Finally, except for **2a** and **2d**, all crystal structures are stabilised by π···π stacking interaction but only the charged methoxymethyl substituted derivative **1a** forms molecular strands.

The nature of the hydrogen bonds involved in the cyclic dimers was analysed with the quantum theory of atoms in molecules (QTAIM). For this purpose **1a** and **2a** were chosen as representatives for the corresponding group of charged and neutral alkoxymethyl-8-hydroxyquinolines. All hydrogen bonds stabilizing the dimers are weak according to the criteria proposed by Rozas and coworkers.[67] The hydrogen bonds Cl1···H2O and Cl1···H1N are stronger than the other hydrogen bonds.

The substitution of 8-hydroxyquinolines with different alkoxy groups in 5-position allows the fine tuning of the packing properties in the solid state. Knowledge about these subtle changes might be useful for the solid state properties of coordination compounds including porous coordination polymers with these molecules or corresponding building units as ligands.[72]

Acknowledgement

The authors thank the Dr.-Erich-Krüger foundation (Germany) at TU Bergakademie Freiberg within the Krüger Research School: Biohydrometallurgical Center for Strategic Elements (BHMZ).

References

1 Y. Song, H. Xu, W. Chen, P. Zhan and X. Liu , Med. Chem. Commun. 6 (2015) 61.
2 J.P. Phillips, Chem. Rev. 56 (1956) 271.
3 M. Albrecht, M. Fiege, O.Osetska, Coord. Chem. Rev. 252 (2008) 812.
4 V. Oliveri, G. Vecchio, Eur. J. Med. Chem. 120 (2016) 252.
5 F. Vögtle and E. Weber, Angew. Chem. 91 (1979) 813; F. Vögtle and E. Weber, Angew. Chem. Int. Ed. 18 (1979) 753.

6 F. Vögtle, H. Sieger, W.M. Müller, Top. Curr. Chem. 98 (1981) 107-161.

7 A. Fernandez-Gutierrez and A. Munoz de la Pena, in Molecular Luminescence Spectroscopy. Methods and Application: Part I; ed. S.G. Schulman, Wiley, 1985; pp 371-546.

8 G. Farruggia, S. Iotti, L. Prod, M. Montalti, N. Zaccheroni, P.B. Savage, V. Trapani, P. Sale and F.I. Wolf, J. Am. Chem. Soc. 128 (2006) 344.

9 J.R. Sheats, H. Antoniadis, M. Hueschen, W. Leonard, J. Miller, R. Moon, D. Roitman and A. Stocking, Science 273 (1996) 884.

10 C.W. Tang, S.A. VanSlyke, Appl. Phys. Lett. 51 (1987) 913.

11 M. Amati and F. Lelj, J. Phys. Chem. A 107 (2003) 2560.

12 G.R. Desiraju, J.J. Vittal, A. Ramanan, Crystal Engineering, World Scientific, Singapore, 2011.

13 Q. Fernando, W.L.W. Ludekens and K. Gnanasoorian, Anal. Chim. Acta 14 (1956) 297.

14 J. H. Burckhalter and R. I. Leib, J. Org. Chem. 26 (1961) 4078.

15 B. Venkataramani, Curr. Sci. 32 (1963) 302.

16 G.R. Chauhan, G.J. Kharadi and K.D. Patel, Orient. J. Chem. 6 (2010) 1431.

17 Stoe & Cie (2009). X-RED and X-AREA. Stoe & Cie, Darmstadt, Germany.

18 Bruker (2007). SMART, SADABS and SAINT. Bruker AXS Inc., Madison, Wisconsin, USA.

19 G.M. Sheldrick, Acta Crystallogr., Sect. A: Found. Crystallogr. 64 (2008) 112.

20 G.M. Sheldrick, Acta Crystallogr., Sect. C: Struct. Chem. 71 (2015) 3.

21 A.L. Spek, Acta Crystallogr., Sect. C: Struct. Chem. 71 (2015) 9.

22 M.A. Spackman and D. Jayatilaka, CrystEngComm 11 (2009) 19.

23 M.A. Spackman and J.J. McKinnon, CrystEngComm 4 (2002) 378.

24 S.K. Wolff, D. J. Grimwood, J. J. McKinnon, M. J. Turner, D. Jayatilaka and M.A. Spackman, CrystalExplorer (Version 3.1), University of Western Australia, 2010.

25 J.J. McKinnon, M.A. Spackman and A.S. Mitchell, Acta Crystallogr., Sect. B: Struct. Sci. 60 (2004) 627.

26 F.P.A. Fabbiani, L.T. Byrne, J.J. McKinnon and M.A. Spackman, CrystEngComm 9 (2007) 728.

27 M.J. Turner, J.J. McKinnon, D. Jayatilaka and M.A. Spackman, CrystEngComm 13 (2011) 1804.

28 Gaussian 09, Revision D.01, M.J. Frisch, G.W. Trucks, H.B. Schlegel, G.E. Scuseria, M.A. Robb, J.R. Cheeseman, G. Scalmani, V. Barone, B. Mennucci, G.A. Petersson, H. Nakatsuji, M. Caricato, X. Li, H.P. Hratchian, A.F. Izmaylov, J. Bloino, G. Zheng, J.L. Sonnenberg, M.Hada, M. Ehara, K. Toyota, R. Fukuda, J. Hasegawa, M. Ishida, T. Nakajima, Y. Honda, O. Kitao, H. Nakai, T. Vreven, J.A. Montgomery, Jr., J.E. Peralta, F. Ogliaro, M. Bearpark, J.J. Heyd, E. Brothers, K.N. Kudin, V.N. Staroverov, T. Keith, R. Kobayashi, J. Normand, K. Raghavachari, A. Rendell, J.C. Burant, S.S. Iyengar, J. Tomasi, M. Cossi, N. Rega, J.M. Millam, M. Klene, J.E. Knox, J.B. Cross, V. Bakken, C. Adamo, J. Jaramillo, R. Gomperts, R.E. Stratmann, O. Yazyev, A.J. Austin, R. Cammi, C. Pomelli, J.W. Ochterski, R.L. Martin, K. Morokuma, V.G. Zakrzewski, G.A. Voth, P. Salvador, J.J. Dannenberg, S. Dapprich, A.D. Daniels, O. Farkas, J.B. Foresman, J.V. Ortiz, J. Cioslowski, and D.J. Fox, Gaussian, Inc., Wallingford CT, 2013.

29 A.D. Becke, J. Chem. Phys. 98 (1993) 5648.

30 P.J. Stevens, F.J. Devlin, C.F. Chablowski and M.J. Frisch, J. Phys. Chem. 98 (1994) 11623.

31 P.C. Hariharan and, J.A. Pople, Theor. Chim. Acta 28 (1973) 213.

32 M.M. Francl, W.J. Pietro, W. J. Hehre, J. S. Binkley, M. S. Gordon, D. J. DeFrees, and J.A. Pople, J. Chem. Phys. 77 (1982) 3654.

33 A. Gavezzotti, Molecular Aggregation, Oxford University Press, Oxford 2007, pp. 199.

34 T. Gruene, H. W. Hahn, A. V. Luebben, F.Meilleur, G. M. Sheldrick J. Appl. Cryst. 47 (2014) 462-466.
35 F.H. Allen and I. J. Bruno, Acta Crystallogr., Sect. B: Struct. Sci. 66 (2010) 380.
36 V.L. Deringer, V. Hoepfner and R. Dronskowski, Cryst. Growth Des. 12 (2012) 1014.
37 F. Biegler-König, J. Schönbohm and D. Bayles, J. Comp. Chem., 2001, 22, 545.
38 J.C. Ortiz and C. Bo, Xaim, Universitat Rovira i Virgili, Tarragona, Spain, 1998.
39 F.H. Allen, O. Kennard, D.G. Watson, L. Brammer, A.G. Orpen and R. Taylor, J. Chem. Soc. Perkin Trans. 2, 1987, S1-19.
40 G.B. Deacon, T. Dierkes, M. Hübner, P.C. Junk, Y. Lorenz and A. Urbatsch, Eur. J. Inorg. Chem, 2011, 4338.
41 W.-S. Loh, M. Hemamalini and H.-K. Fun, Acta Crystallogr., Sect. E: Struct. Rep. Online, 2010, 66, o2907.
42 K. Mereiter (2009) Private communication to the Cambridge Structural Database, deposition number CCDC 729803.
43 M. Damous, G. Dénès, S. Bouacida, M. Hamlaoui, H. Meraziga and J.-C. Darand, Acta Crystallogr., Sect. E: Struct. Rep. Online, 2013, 69, o1458.
44 J.M.S.Skakle, J.L.Wardell and S.M.S.V.Wardell, Acta Crystallogr., Sect. C: Cryst. Struct. Commun., 2006, 62, o312.
45 R. Bishop, CrystEngComm, 2015, 17, 7448
46 E. Arunan, G.R. Desiraju, R.A. Klein, J. Sadlej, S. Scheiner, I. Alkorta, D.C. Clary, R.H. Crabtree, J.J. Dannenberg, P. Hobza, H.G. Kjaergaard, A.C. Legon, B. Mennucci and D.J. Nesbitt, Pure Appl. Chem., 2011, 83, 1637.
47 G.R. Desiraju and T. Steiner, The weak hydrogen bond, Oxford University Press, New York, 1999.
48 M. Nishio, Y. Umezawa, H. Suezawa and S. Tsuboyama in The Importance of Pi-Interactions in Crystal Engineering: Frontiers in Crystal Engineering, ed. E.R.T. Tiekink and J. Zukerman-Schpector, Wiley, 2012, pp. 1-39.
49 C.R. Martinez and B.L. Iverson, Chem. Sci., 2012, 3, 2191.
50 T. Steiner, Angew. Chem. 2002, 114, 50; T. Steiner, Angew. Chem. Int. Ed., 2002, 41, 48.
51 P. Roychowdhury, B.N. Das and B.S. Basak, Acta Crystallogr., Sect. B: Struct. Crystallogr. Cryst. Chem., 1978, 34, 1047.
52 T. Banerjee and N.N. Saha, Acta Crystallogr., Sect. C: Cryst. Struct. Commun., 1986, 42, 1408.
53 R. Castañeda, S.A. Antal, S. Draguta, T.V. Timofeeva and V.N. Khrustalev, Acta Crystallogr., Sect. E: Struct. Rep. Online, 2014, 70, o924.
54 V. Krishnakumar, R. Nagalakshmi and P. Janaki, Spectrochim. Acta, Part A, 2005, 61, 1097.
55 M. Szala, J.E. Nycz and G.J. Malecki, J. Mol. Struct. 2014, 1071, 34.
56 J.-Y. Zhao, Z.-Y. Zhou, Z.-M. Su, Y.-Z. Xie, G.-Y. Sun and X. Wu, Chin. J. Chem., 2006, 24, 724.
57 M. Amati, S. Belviso, P. L. Cristinziano, C. Minichino, F. Lelj, I. Aiello, M. La Deda and M. Ghedini, J. Phys. Chem. A, 2007, 111, 13403.
58 Z.-Y. Zhou, G.-G. Shan, Y.-L. Zhu, X.J. Yu, Y.-H. Dong and J.-Y. Zhao, J. Struct. Chem., 2009, 50, 606.
59 Y.-H. Liu, S.-C. Lan and C.-R. Li, Spectrochim. Acta, Part A, 2013, 112, 257.
60 S.-C. Lan, Y.-H. Liu, Spectrochim. Acta, Part A, 2015, 139, 49.
61 R.F. W. Bader, Atoms in Molecules, Clarendon Press, Oxford, 1994.
62 R.J. Gillespie, J. Chem. Educ., 2001, 78, 1688.
63 R.J. Gillespie and P.L.A. Popelier, Chemical Bonding and Molecular Geometry, Oxford University Press, New York, 2001.
64 R.F.W. Bader and H. Essén, J. Chem. Phys., 1984, 80, 1943.
65 U. Koch and P. L. A. Popelier, J. Phys. Chem., 1995, 99, 9747.

66 G. W. Fester, J. Wagler, E. Brendler, U. Böhme, D. Gerlach and E. Kroke, J. Am. Chem. Soc., 2009, 131, 6855.
67 I. Rozas, I. Alkorta and J. Elguero, J. Am. Chem. Soc., 2000, 122, 11154.
68 S.J. Grabowski, in The Quantum Theory of Atoms in Molecules, ed. C. F. Matta, R. J. Boyd, Wiley-VCH, Weinheim 2007, pp. 453-469.
69 E. Espinosa, E. Molins and C.Lecomte, Chem. Phys. Lett., 1998, 285, 170.
70 E. Espinosa, C. Lecomte and E.Molins, Chem. Phys. Lett., 1999, 300, 745.
71 J. Netzel and S. van Smaalen, Acta Crystallogr., Sect. B: Struct. Sci., 2009, 65, 624.
72 L.R. MacGillivray (ed.), Metal-Organic Frameworks, Wiley, Hoboken, 2010.

Highlights:

- Alkoxymethyl substituted derivatives of 8-hydroxyquinoline were synthesised.
- Protonated and neutral forms were characterised by single X-Ray.
- Hirshfeld surface analyses were applied to analyse hydrogen bonds.
- Topological analysis delivers details about the strength of hydrogen bonds.